Morphological evolution in the electrodeposition of the Pb-Sn binary system

Bin Sun, Xian-Wu Zou,* and Zhun-Zhi Jin

Department of Physics, Wuhan University, Wuhan 430072, China

(Received 26 May 2003; revised manuscript received 10 December 2003; published 14 June 2004)

Morphological evolution in the electrodeposition of Pb-Sn binary system is studied. As the second component increases, the morphology of the codeposit changes from dendrite to ramification, to dense branch, and finally to fractal structure, respectively. The evolution arises from the influence of crystallographic texture, which leads to a splitting of dendritic tips and the formation of ramified morphology. This work provides direct evidence to explore the crystallographic influence on the morphological evolution in electrodeposition.

Quasi-two-dimensional electrochemical deposition (ECD) is an ideal system to investigate the nonequilibrium growth process [1]. During the past two decades, electrodepositions of unitary metals such as zinc, copper, and silver have been studied extensively. Great efforts have been directed to explore the underlying mechanisms for the different morphologies such as dendrite, fractal, etc. [2–4]. In general, it is accepted that the transport mechanism, interface kinetics, and crystallographic orientation are the three essential ingredients in determining the morphologies of aggregates [1–5]. In earlier work by other researchers, a great number of experiments and models were focused on the investigation of these mechanisms. For instance, it was discovered that with the variance of some basic parameters (i.e., the electrolyte concentration, applied voltage, or cell current), the transport process was changed and very different patterns were obtained. Furthermore, it was found that the electrochemical reaction at the growing interface also had an influence on the morphological selection and transition [6,7].

However, the influence of chemical compositions of the electrolyte solution received less attention in previous ECD experiments and was much less understood. In fact, the composition of the electrolyte solution plays an important role in changing both the growth environment and interface kinetics in the electrodeposition [8,9]. Kuhn and Argoul [10] have shown that the presence of oxygen and alkaline cations in the zinc salt solution affects the morphology of the deposit. Trigueros, Sagues, and Claret [11] have investigated the effect of the inert electrolyte sodium sulphate on copper electrodeposition and have obtained a novel morphology. Similar phenomena have been observed in other complex solutions, such as a solution of copper sulphate with nondepositing species (e.g., organic additives).

In previous studies of morphological transitions in electrochemical deposition, the deposit was pure metal, such as Zn and Cu. In this Brief Report, we designed the electrodeposition experiments with a binary solution in which two types of metal cations codeposit and form two-component deposits. As the proportion of one cation to the other in solution changed, a series of distinct morphologies appeared successively. We investigated the underlying

mechanisms of this interesting morphology evolution and found that the morphological transition arose from the variation of the crystallographic texture of the deposits with the composition of the electrolyte solution. This result presents direct experimental evidence of the crystallographic influence on the morphologies of aggregates.

According to thermodynamics, the condition for codeposition of two kinds of metallic ions M_1 and M_2 is that their standard potentials ϕ_0^1 and ϕ_0^2 should be close [12]. The Pb-Sn system is one of the very rare systems that meets this condition. Pb and Sn have a standard potential of −0.126 and −0.136 V, respectively. Therefore we chose Pb and Sn as two types of cations in our solution. In order to avoid a reaction between Pb and Sn, the electrolyte with the same anion, $Pb(BF_4)_2$ and $Sn(BF_4)_2$, was selected.

The electrochemical deposition of the Pb-Sn codeposit was carried out in the electrolyte solution sandwiched by two glass plates. The experimental device is illustrated in Fig. 1. The size of the upper glass plate was 4 cm in length and 2 cm in width. The thickness of the electrolyte solution was controlled by the mica spacer (100 μm in our experiment). The cathode was made of platinum plate, whose width was the same as that of the glass plate. The anode was graphite plate, being an inert material, thereby avoiding a chemical reaction with the electrolyte solution. The experimental parameters were set as follows: The total cation concentration in the electrolyte solution was 0.7 mol, the applied voltage was 2 V, and the distance between two glass plates 100 μm. The electrodeposition was performed at room temperature (approximately 20 °C).

The morphologies of the deposits were observed by an optical microscope and recorded by a digital camera as shown in Fig. 1. The analysis on the microstructure were conducted on the JEOL JXA-8800R (Tokyo, Japan) scanning electron probe microanalyzer (EPMA). Since the deposits were very thin and brittle, the preparation of samples for texture examination demanded great attention to detail. Several special methods were used. The deposit was firstly segregated from the glass plate by the water-floating method [13] and was then mounted in the aluminum tube with a resin-agent mixture [14]. After solidification, the deposit was ground carefully with abrasive cloth until the longitudinal section was revealed. It was then polished and etched. The Pb-Sn alloy was very soft and risked being easily distorted

---

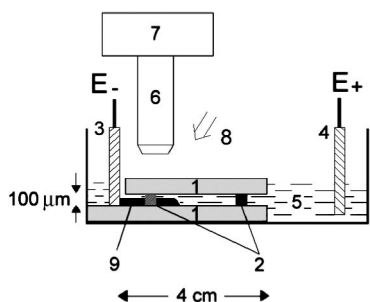*Corresponding author. Electronic address: xwzou@whu.edu.cn

FIG. 1. A schematic diagram of the experiment setup: (1) the glass plate made of a microscope slide, (2) spacers made of mica sheets, (3) platinum cathode, (4) graphite anode, (5) electrolyte solution, (6) microscope, (7) digital camera, (8) lights, and (9) deposit.

during the grinding process. A lubrication was added to reduce the distortion during grinding. To remove the distorted layer, a special etching reagent consisting of hydrogen peroxide and glacial acetic acid in a ratio of 1:1 was used [15]. This etching-polish process was repeated several times. Additionally, it was noted that the Pb-Sn alloy was unstable in the microstructure and that recrystallization may take place at a higher temperature or in a longer period [16,17]. Solidification of resin took about 6 h. To monitor the recrystallization process a set of reference samples was prepared by mounting samples with half-melting paraffin wax. The mounting temperature was about 40°C and solidification time about 15 min. We found that the variation of the texture of the deposit could not be observed in the first 30 h for the Pb-Sn deposits with the Sn content ranging from 10 to 70 at.% at room temperature by using a metallographic microscope (Nikon, EPIHPOT300) with magnification of 1000×. A slight change in texture occurred after about 50 h. This result is consistent with the finding of Gupta, Vieregge, and Gust [17], which shows that the microstructure of the Pb-Sn alloy displays a minor change after being annealed for 64 h at 40°C [17]. In our experiments, the preparation of samples and microstructure analysis was completed within 10 h, so the observed texture can be assumed as the original texture.

Figure 2 shows the evolution of the deposit morphologies as the proportion of Pb^{2+} to Sn^{2+} varies. In the case of the pure Pb [Fig. 2(a)], the deposits are dendrites, which consist of straight backbones with a considerable number of regular side branches. When 10 at.% Sn is added [Fig. 2(b)], the deposit still retains the dendritic characteristics, but the growing tip begins to split, which leads to variation in growth directions. With the increase of the Sn concentration [Figs. 2(c) and 2(d)], more and more tips are split. The deposit grows in a tip-splitting way and no longer maintains the main stem. Furthermore, the growth of the side branches also becomes unstable, and the angle between the backbone and side branches is arbitrary in comparison with the angle for the pure Pb dendrites. Figure 2(e) shows the morphology of the deposit obtained from the electrolyte solution with 60 at.% $Pb(BF_4)_2 + 40$ at.% $Sn(BF_4)_2$. It can be seen that the deposit loses the features of dendritic growth in macroscopic scale. However, a close observation reveals that the deposit still consists of many short dendrites, which are formed by frequent tip splitting during dendritic growth. When the content of Sn reaches 50 at.% [Fig. 2(f)], the deposit has a typical dense branch morphology (DBM). This kind of morphology possesses the characteristics of both dendritic and fractal morphology. The backbones possess the dendritic feature, and the lateral branches are typical open fractal structures. As the Sn^{2+} concentration reaches 70% [Fig. 2(g)], the deposit morphology becomes the standard fractal style. The evolution of the morphologies from Fig. 2(a) to 2(g) corresponds to the morphological transition from dendrites to fractals as more and more Sn^{2+} ions are added into the $Pb(BF_4)_2$ solution. The morphology evolution from Fig. 2(j) to 2(g) shows a similar variation of growth morphologies with the increase of Pb^{2+} ions in the $Sn(BF_4)_2$ solution. Figure 2(j) presents the irregular dendritic morphology of the pure Sn deposit. The main branch is somewhat tortuous and side branches are uneven. As the Pb^{2+} ion concentration increases [Figs. 2(i) and 2(h)], the tip of the main branch splits more frequently and the morphology of the deposit changes into fractals.

Therefore, the morphological evolution in the Pb-Sn ECD system can be described as follows: as the content of the second cation component increases from zero to eutectic composition (74 at.% Sn), the morphology of the codeposit changes successively from standard dendrites to ramifications, to dense branches, and finally to fractals. This transition essentially arises from tip splitting during the course of deposit growth, and the tip splits more frequently as the con-
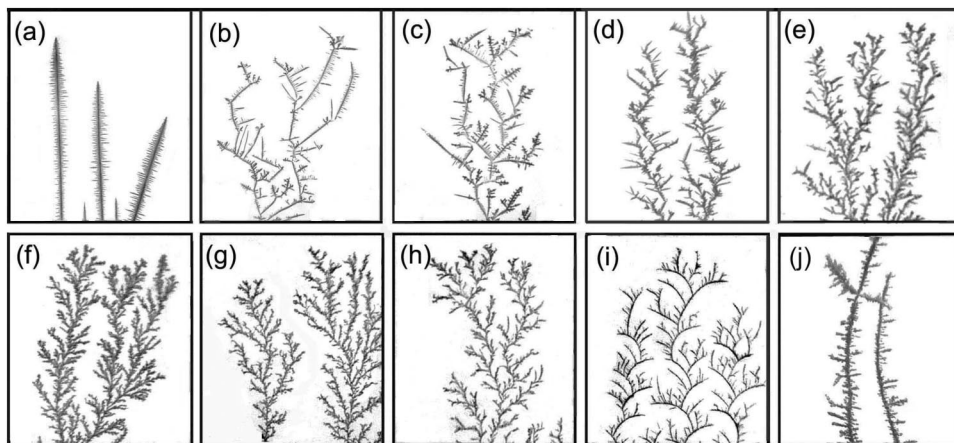

FIG. 2. Morphology evolution (50× magnification)in the electrodeposition of $Pb(BF_4)_2 + Sn(BF_4)_2$ system as the Sn content varies. Cell thickness: 100 μm. (a) Pure Pb, (b) 10 at.% Sn, (c) 20 at.% Sn, (d) 30 at.% Sn, (e) 40 at.% Sn, (f) 50 at.% Sn, (g) 70 at.% Sn, (h) 80 at.% Sn, (i) 90 at.% Sn, and (j) pure Sn.
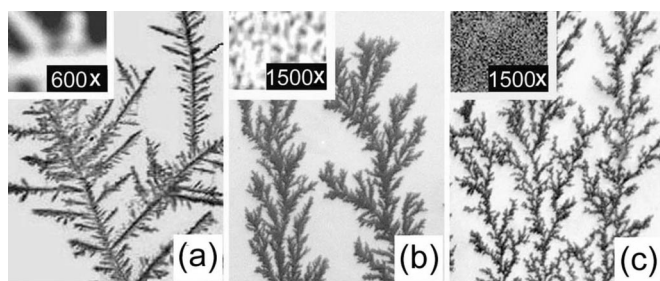
FIG. 3. Morphologies (200× magnification) of the typical dendrites, dense branches, and fractal structures. Cell thickness: 50 μm. (a) 10 at.% Sn, (b) 50 at.% Sn, and (c) 70 at.% Sn. The insets are the corresponding scanning electron microscope (SEM) back scattering electron images of the texture of the branch. In each inset, the white and gray areas represent lead and tin, respectively. The compositions of the deposits measured by EPMA are (a) 9.46, (b) 53.27, and (c) 72.51 at.% Sn.

tent of the second component increases. In the previous studies of thin layer electrodeposition, the formation of tip splitting is mainly attributed to the instability of the growing interface. The origin of the instability varies for different systems. It may be associated with the impurity effect in interfacial kinetics, chemical transport, or other special non-linear boundary conditions [6,18–20]. Recently, it was discovered by others that the convection phenomenon, caused by concentration gradient and local charges, plays a more important role in determining the growth morphology [6,20]. However, in the present experimental system, the instability was not caused by any of these reasons since all of the experimental parameters were constant except for the proportion of the two types of metal ions. It is reasonable to conclude that this transition in morphology comes from the variation of the composition of the deposit rather than from other mechanisms.

How does the variation in the composition of the deposit lead to the morphological evolution for the Pb-Sn deposit? We investigated the relationship between the morphology and texture of the deposit and attempted to understand the formation mechanism of the morphologies. Figure 3 shows three typical morphologies of Pb-Sn deposits: dendrites [Fig. 3(a)], dense branches [Fig. 3(b)], and fractal structures [Fig. 3(c)]. Corresponding to Figs. 3(a)–3(c), the proportion of Sn^{2+} in solution was 10, 50, and 70 at.%, respectively. These deposits were prepared by using an electrolyte cell with a thickness of 50 μm. The microstructures of the deposits were observed using metallographic methods and the corresponding textures are displayed in the insets of Fig. 3. In Fig. 3(a), when the 10 at.% Sn is added, the texture of the cross section of the branch shows the aggregation of crystal grains of Pb-based solid solution with the size of the order of 10 μm and the morphology of the deposit retaining the main feature of the dendrites. As the Sn content increases to 50 at.% the texture of the cross section of the branch becomes pseudoeutectic and the mean size of the Pb crystal grains is about 2 μm. Correspondingly, the morphology of

the deposit changes into dense branches, as shown in Fig. 3(b). When the Sn content reaches 70 at.%, close to the eutectic composition (74 at.% Sn), the texture of the cross section of the branch is still pseudoeutectic, but the size of the crystal grains is much smaller (about 300 nm). The dispersion of the crystal grains is also much larger than the dispersion for low Sn concentrations. In the case of the eutectic composition, growth and ramification of the branches are completely random, and the morphology is the typical fractal structure [see Fig. 3(c)].

Pb-Sn alloy is a typical binary alloy with limited mutual solubility. According to the Pb-Sn phase diagram, when the alloy composition is eutectic, normal texture is a random mixture of the crystals of Pb and Sn, as shown in the inset of Fig. 3(c). When the composition is between eutectic and solid solubility, the texture is that of larger Pb (or Sn) crystals and smaller Sn (or Pb) crystals, as shown in the inset of Fig. 3(b). Petersson and Ahlberg have investigated the morphology and texture of Pb-Sn alloy obtained from electrodeposition and shown that the texture of the alloy approximately meets the above rule [21]. In the present case, the randomness is due to the crystallographic microstructure. The deposit of pure Pb appears to be regular dendrites with strong anisotropy. When low concentration Sn is added, Sn atoms are embedded in the crystal lattice of Pb and form a Pb-based solid solution. Once the content of Sn exceeds the solubility of Sn in Pb, the superfluous Sn atoms precipitate out and form small Sn crystal grains in the deposit. Mixed growth of the Pb and Sn crystal grains weakens the preferred orientational growth and leads to tip splitting of the branches. With the increase of the Sn content the texture of the deposit changes into pseudoeutectic phase where the Pb crystal grains are mixed with more and more Sn grains and the sizes of the grains become smaller and smaller. Thus the mixture with large dispersity breaks the intrinsic anisotropy of crystal growth and allows the randomness to become the dominant factor in the growth of the deposits.

In summary, our study of the electrochemical deposition in a Pb-Sn binary solution has provided direct evidence about crystallographic influence on morphological evolution in electrodeposition. As the proportion of the two kinds of metallic ions varies, the morphology of the deposit evolves from dendrites to fractal structures. These morphological variations result from the influence of the composition of the Pb-Sn solution on the crystallographic texture. The single phase (pure metal or solid solution) in the texture of lead (or tin) dendrites induces the preferred orientational growth. The pseudoeutectic texture consists of a random mixture of the crystal grains of Pb and Sn. It destroys the preferred orientational growth and causes the tips to split, leading to the formation of a series of ramified morphologies.

[1] P. Meakin, *Fractal, Scaling and Growth far from Equilibrium* (Cambridge University Press, New York, 1998).

[2] V. Fleury, Nature (London) **390**, 145 (1997).

[3] M. Haataja and D. J. Srolovitz, Phys. Rev. Lett. **89**, 215509 (2002).

[4] G. Marshall, E. Mocskos, F. V. Molina, and S. Dengra, Phys. Rev. E **68**, 021607 (2003).

[5] C. Leger, J. Elezgaray, and F. Argoul, Phys. Rev. E **61**, 5452 (2000).

[6] F. Sagues, M.-Q. Lopez-Salvans, and P. Claret, Phys. Rep. **337**, 97 (2000).

[7] M. Wang *et al.*, Phys. Rev. Lett. **86**, 3827 (2001).

[8] A. Kuhn and F. Argoul, Phys. Rev. E **49**, 4298 (1994).

[9] M.-Q. Lopez-Salvans, F. Sagues, J. Claret, and J. Bassas, J. Electroanal. Chem. **421**, 205 (1997).

[10] A. Kuhn and F. Argoul, Fractals **1**, 451 (1993).

[11] P. P. Trigueros, F. Sagues, and J. Claret, Phys. Rev. E **49**, 4328 (1994).

[12] A. J. Bard and L. R. Faulkner, *Electrochemical Methods: Fundamentals and Applications* (Wiley, New York, 1980).

[13] Segregation of samples: after the deposit grew, the cathode and then the upper glass plate were removed. It was noted that, due to surface tension, the fragile deposit tended to shrink and be disturbed when the upper glass plate was removed. Yet intact branch deposits could be obtained by repeating growth experiments. The success rate here was about 10%. We then carefully placed the under glass plate with the deposit into a bath of water. Because of surface tension, the deposit floated on the water surface, the glass plate sinking to the bottom. In this way we segregated the samples from the glass plates without damage. Then the deposit gradually sank by disturbing the water surface. Meanwhile, a square plastic film, 2 cm in length, was placed at the bottom of the bath, allowing the deposit to fall on the plastic film.

[14] Mounting of samples: the deposit sank to a plastic film sitting at the bottom of the bath. The film with the deposit was then taken out of the water, and was dried in the air. An aluminous tube, 1.5 cm in diameter and 1.5 cm in length, was put on the plastic film to enclose the deposit on the film. Then a mixture of ethoxyline resin and solidified agent was poured into the aluminous tube. After 6 h, the sample was mounted on the resin.

[15] C. J. Smithells, *Metals Reference Book*, 5th ed. (Butterworths, London, 1976).

[16] Walman Benicio de Castro, Manuel de Lucena Maia, Claudio Shyinti Kiminami, and Claudemiro Bolfarini, Mater. Sci. Eng., A **304–306**, 255 (2001).

[17] D. Gupta, K. Vieregge, and W. Gust, Acta Mater. **47**, 5 (1999).

[18] M. Wang and N. B. Ming, Phys. Rev. Lett. **71**, 113 (1993).

[19] X. Tong, C. Beckermann, A. Karma, and Q. Li, Phys. Rev. E **63**, 061601 (2001).

[20] G. Gonzalez, G. Marshall, F. Molina, and S. Dengra, Phys. Rev. E **65**, 051607 (2002).

[21] I. Petersson and E. Ahlberg, J. Electroanal. Chem. **485**, 166 (2000).